Supporting information

Stable and tunable plasmon resonance of molybdenum oxide nanosheets from ultraviolet to near-infrared region for ultrasensitive surface-enhanced Raman analysis

*Jinhu Wang[a], Yinhua Yang[b], Hua Li[b], Jun Gao[c], Ping He[c], Liang Bian[d], Faqin Dong[d] , and Yi He[*a]*

a. State Key Laboratory of Environment-friendly Energy Materials, Sichuan Co-Innovation Center for New Energetic Materials, School of National Defence Science & Technology, Southwest University of Science and Technology, Mianyang, 621010, P. R. China.

b. Materials Characterization & Preparation Center, Southern University of Science and Technology, Shenzhen 518055, China.

c. School of Materials Science and Engineering, Southwest University of Science and Technology, Mianyang, 621010, P.R. China.

d. Key Laboratory of Solid Waste Treatment and Resource Recycle, Ministry of Education, State Key Laboratory Cultivation Base for Nonmetal Composites and Functional Materials, Southwest University of Science and Technology, Mianyang 621010, Sichuan, China.

*Corresponding author: Prof. Dr. Yi He, Email: yhe2014@126.com.

The Raman enhancement factors (EFs) are calculated by the following equation[S1]:

$$EFs=(I_{SERS}/N_{SERS})/ (I_{bulk}/N_{bulk})$$

where I_{bulk} and I_{SERS} are Raman intensities of bulk dye and in the SERS experiments, N_{SERS} and N_{bulk} are the amounts of dyes in the SERS experiments and bulk measurements, respectively. N_{SERS} and N_{bulk} can be estimated according to the equations:

$$N_{SERS}=CVN_AA_{Raman}/A_{sub}$$

$$N_{bulk}=\rho hA_{Raman}N_A/M$$

where C is the concentration of Raman dye (10 pM), N_A is the Avogadro constant, V is the volume of the droplet, A_{Raman} is the laser spot area, A_{sub} is the effective area of the substrate, ρ and M are density and molecular weight of Raman dye (1.15 g cm^{-3} and 479.02 g mol^{-1}), h is the confocal depth of the laser beam into bulk crystal (h=21 μm).

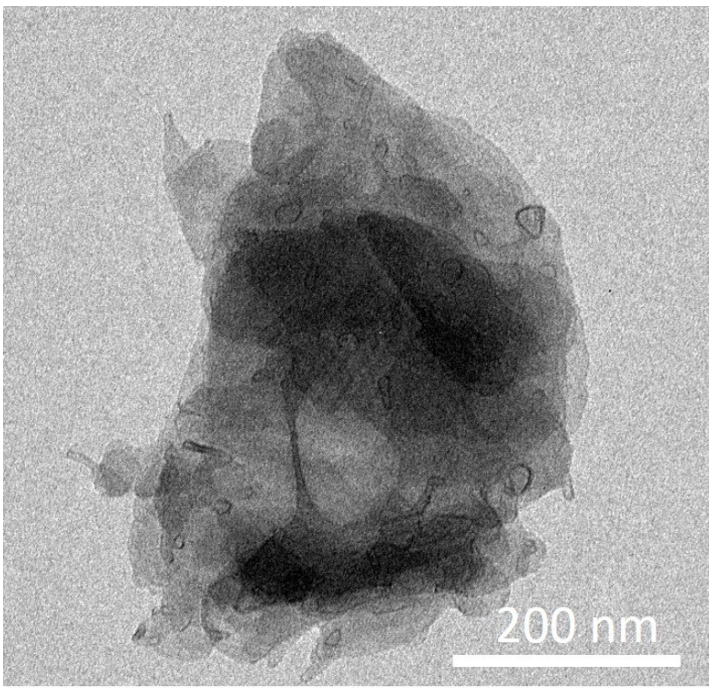

Fig. S1. TEM image of MoO_3 nanosheets.

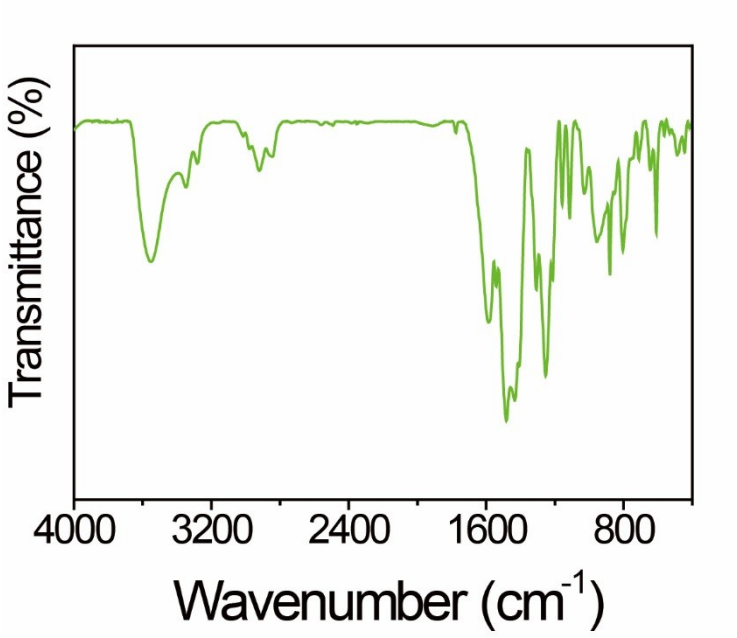

Fig. S2. FTIR spectrum of PDA that is prepared by auto-oxidation of dopamine at pH 8.5.

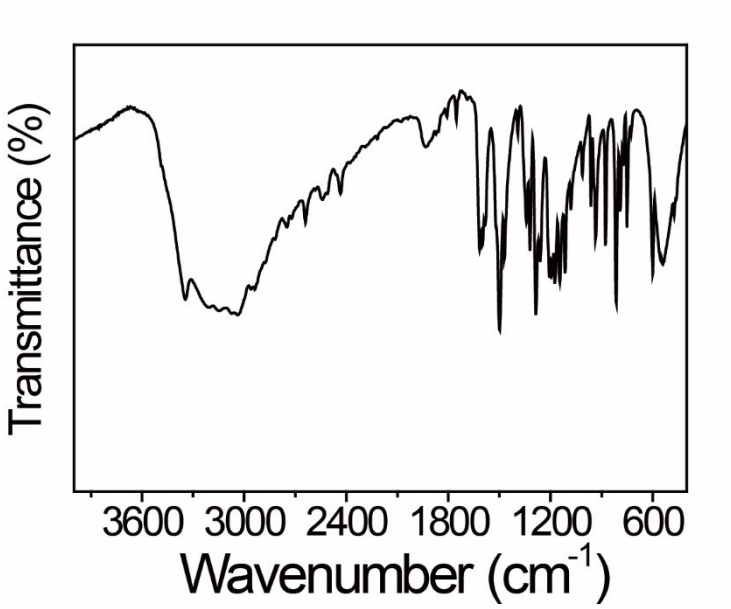

Fig. S3. FTIR spectrum of dopamine.

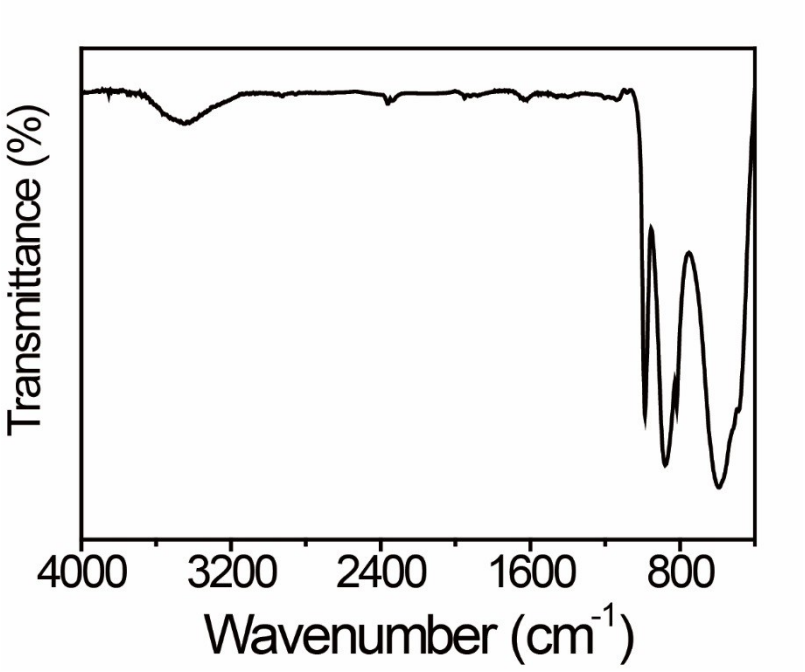

Fig. S4. FTIR spectrum of MoO_3 nanosheets.

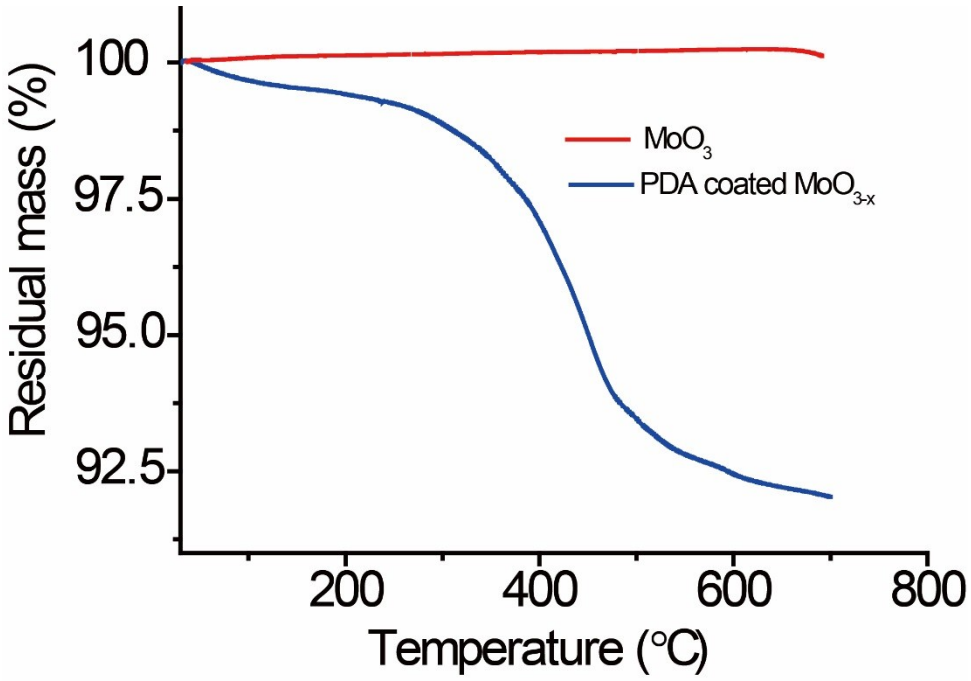

Fig. S5. TGA curves of MoO_3 and MoO_{3-x} nanosheets measured in nitrogen atmosphere.

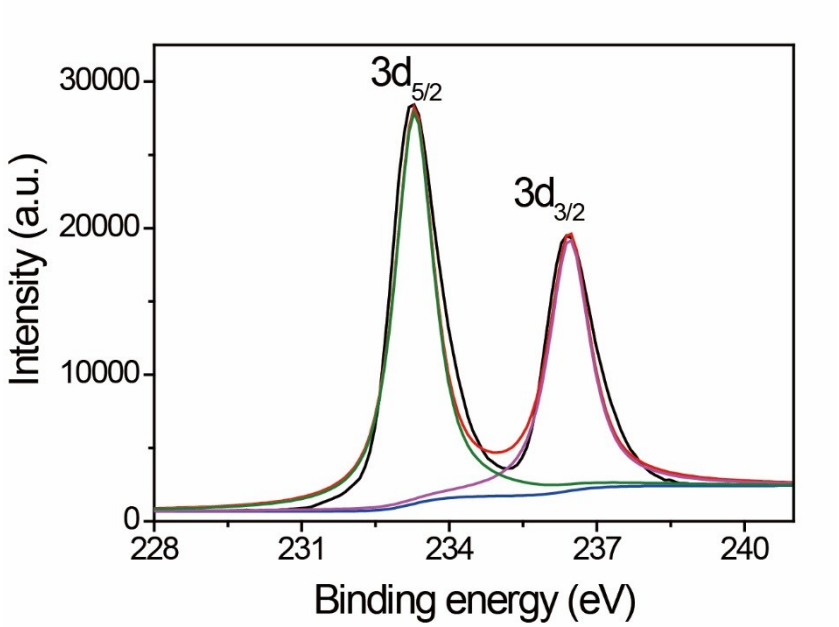

Fig. S6. High-resolution XPS spectra of Mo3d of MoO_3 nanosheets.

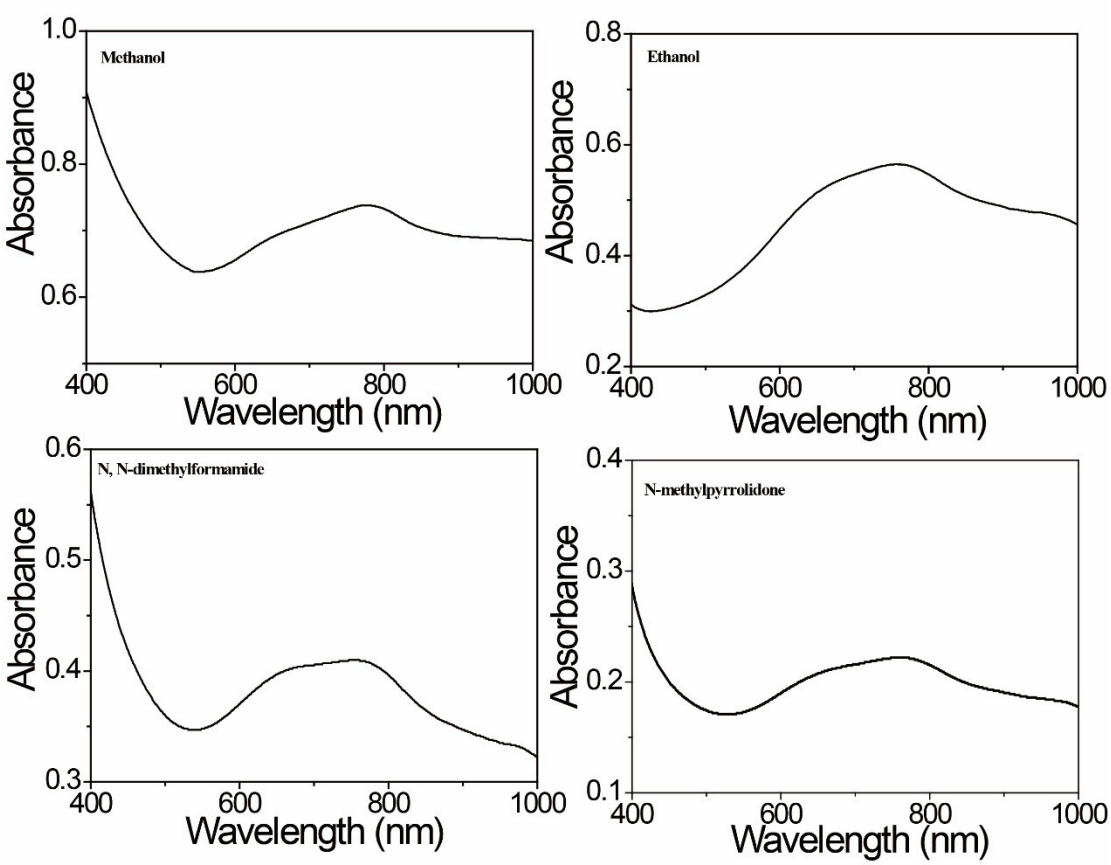

Fig. S7. UV-Vis-NIR spectra of MoO_3 nanosheets dispersed in different solvents.

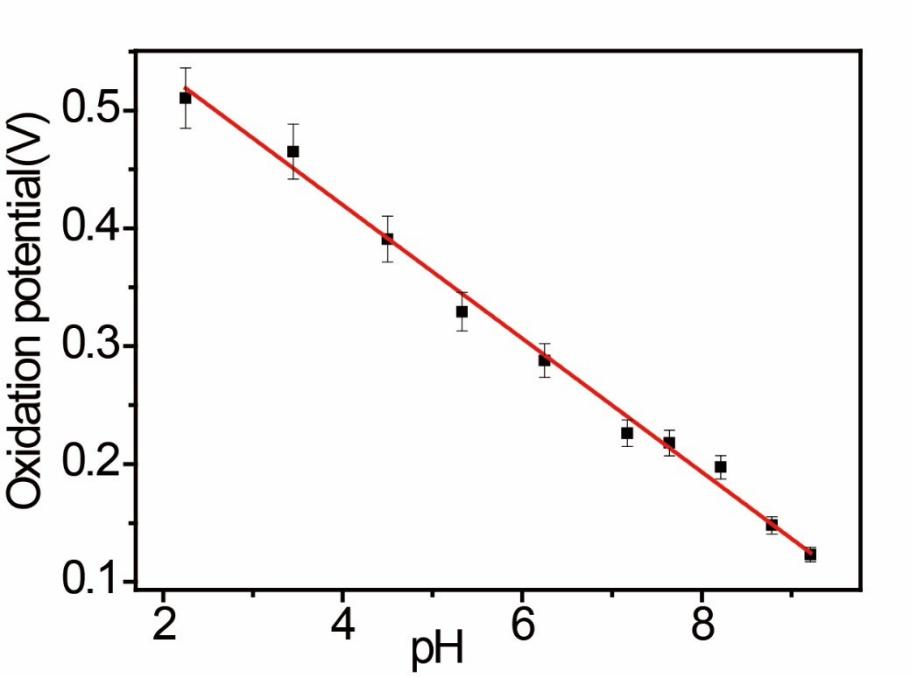

Fig. S8. pH-dependent oxidation potential of dopamine.

Electrochemical measurements were carried out through cyclic voltammetry (CV) in the mixture solution of 0.1 M KCl and 1 mM dopamine under different pH values, and the oxidation potential peaks of dopamine at different pH values are collected. The relationship between oxidation potential and pH value is plotted in Fig. S8. The scan rate in CV is 0.1 V s^{-1}, and the potential range is between -1.0 V and +1.0 V.

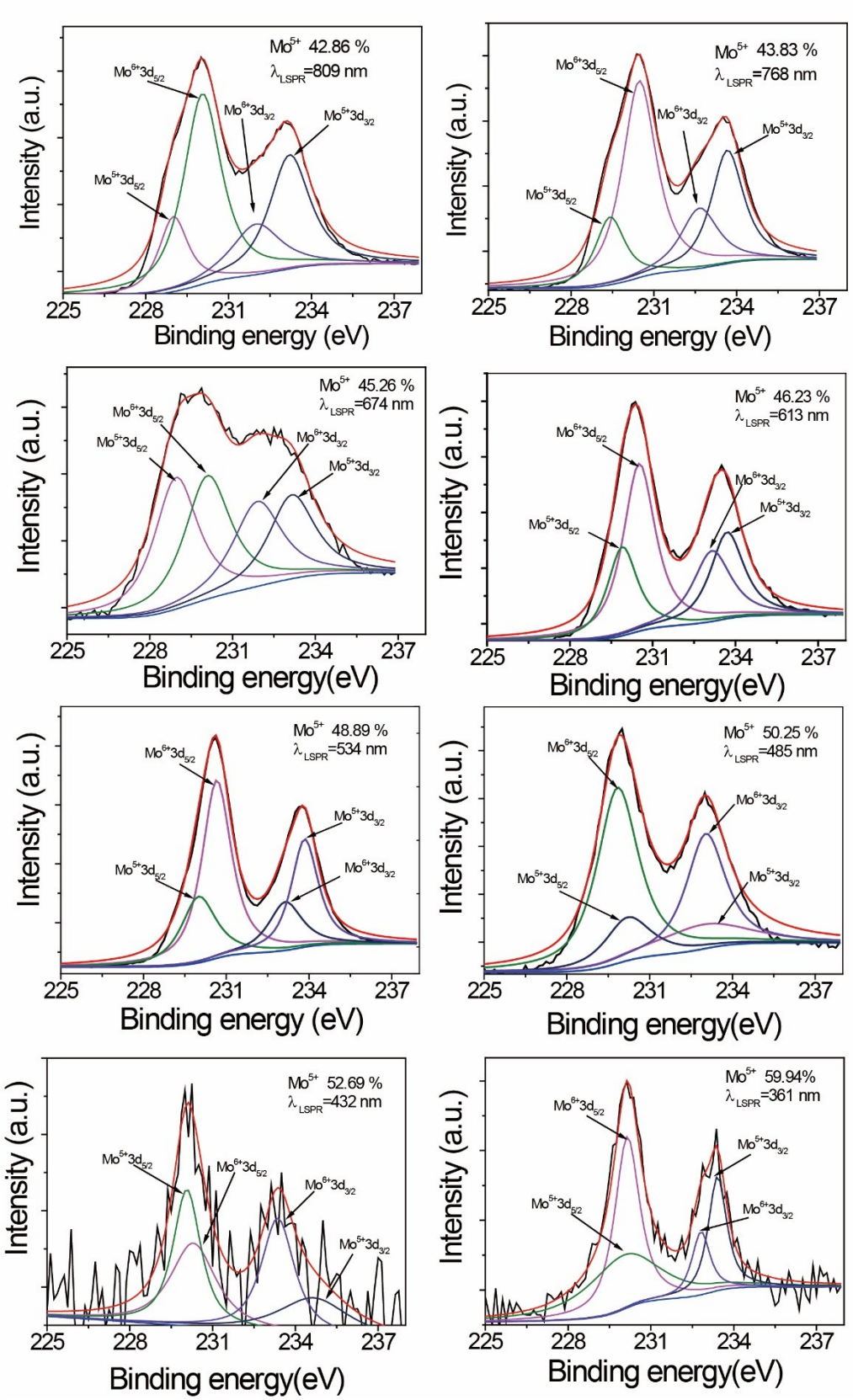

Fig. S9. High-resolution XPS of Mo 3d of PDA-coated MoO_{3-x} nanosheets with different LSPR peaks.

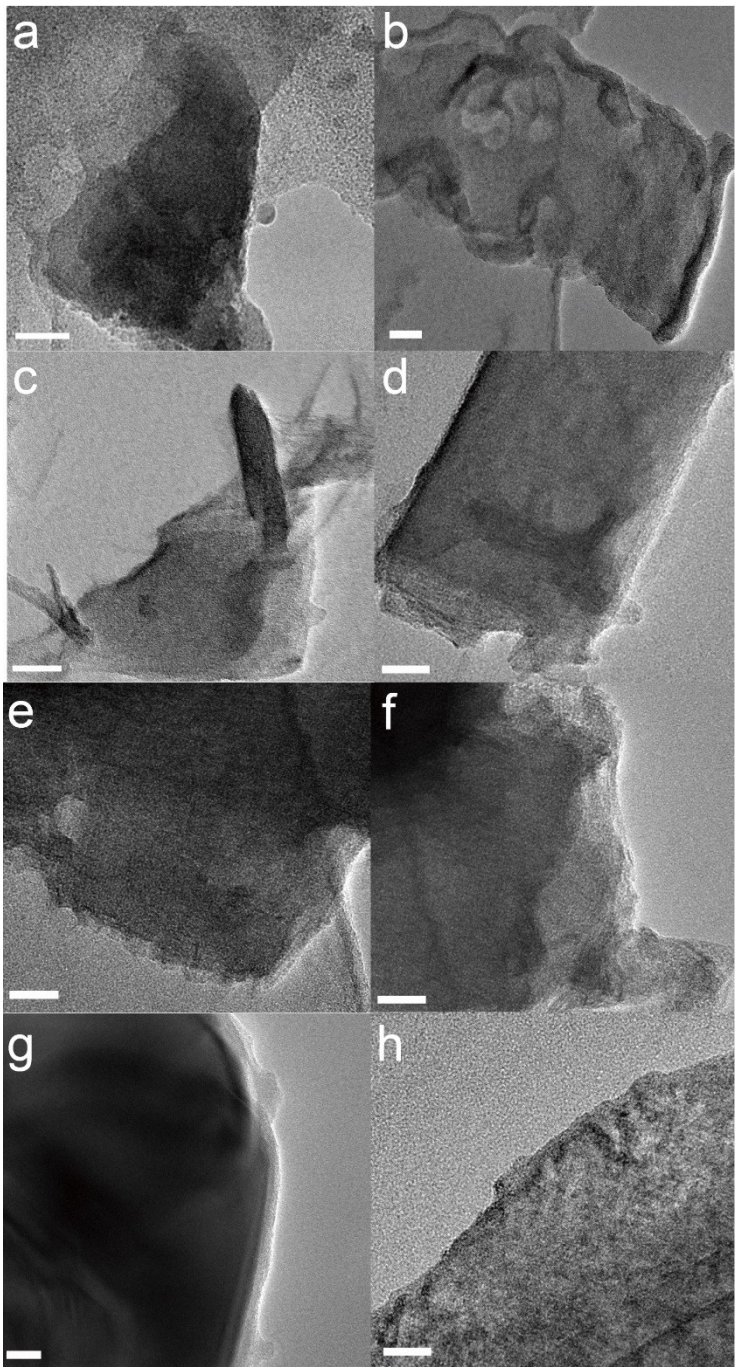

Fig. S10. TEM images of MoO_3 nanosheets with different LSPR peaks (scale bar, 20 nm): a) 809 nm, b) 768 nm, c) 674 nm, d) 613 nm, e) 534 nm, f) 485 nm, g) 432 nm, and h) 361 nm.

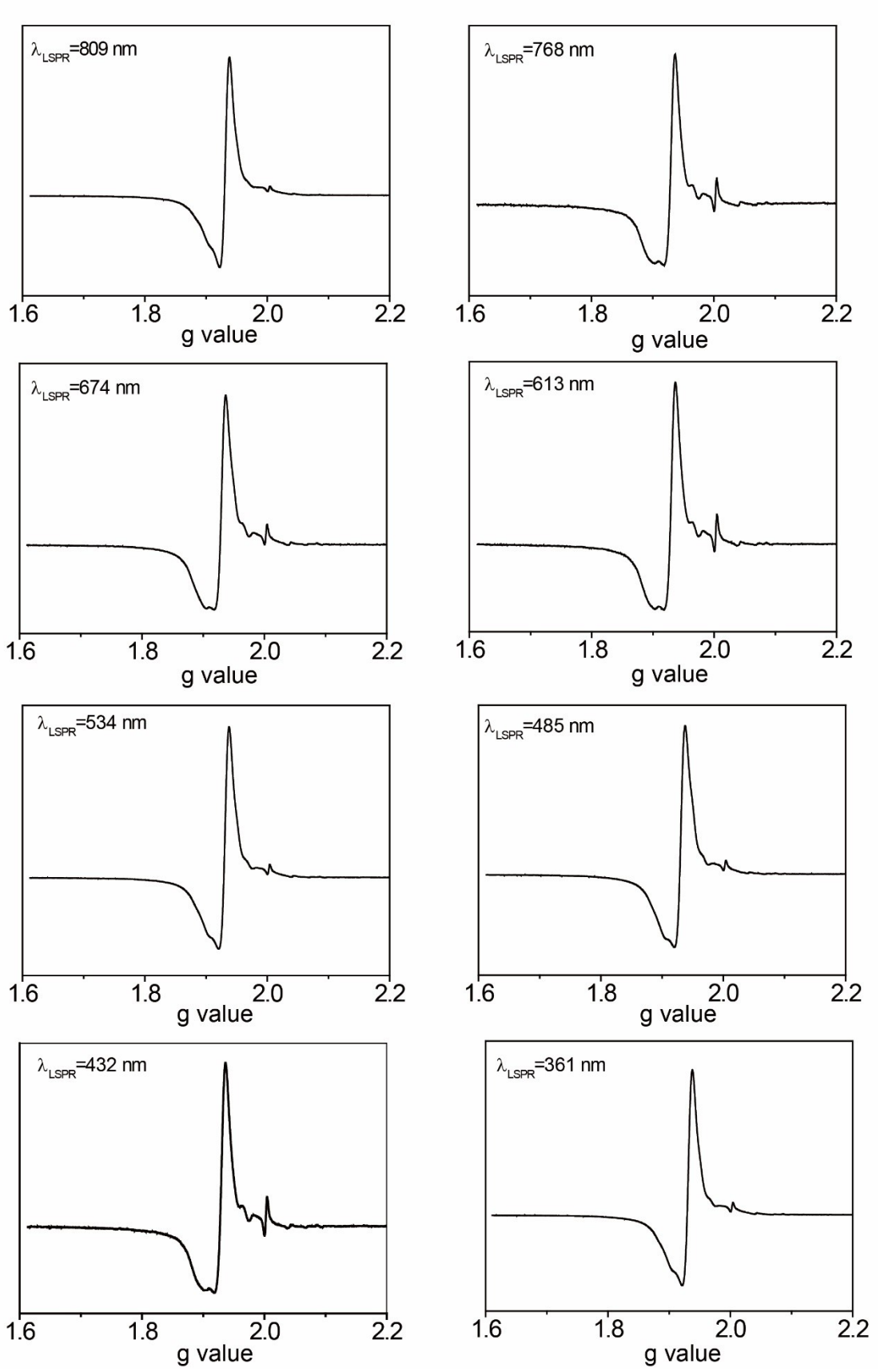

Fig. S11. EPR spectra of MoO_3 nanosheets with different LSPR peaks.

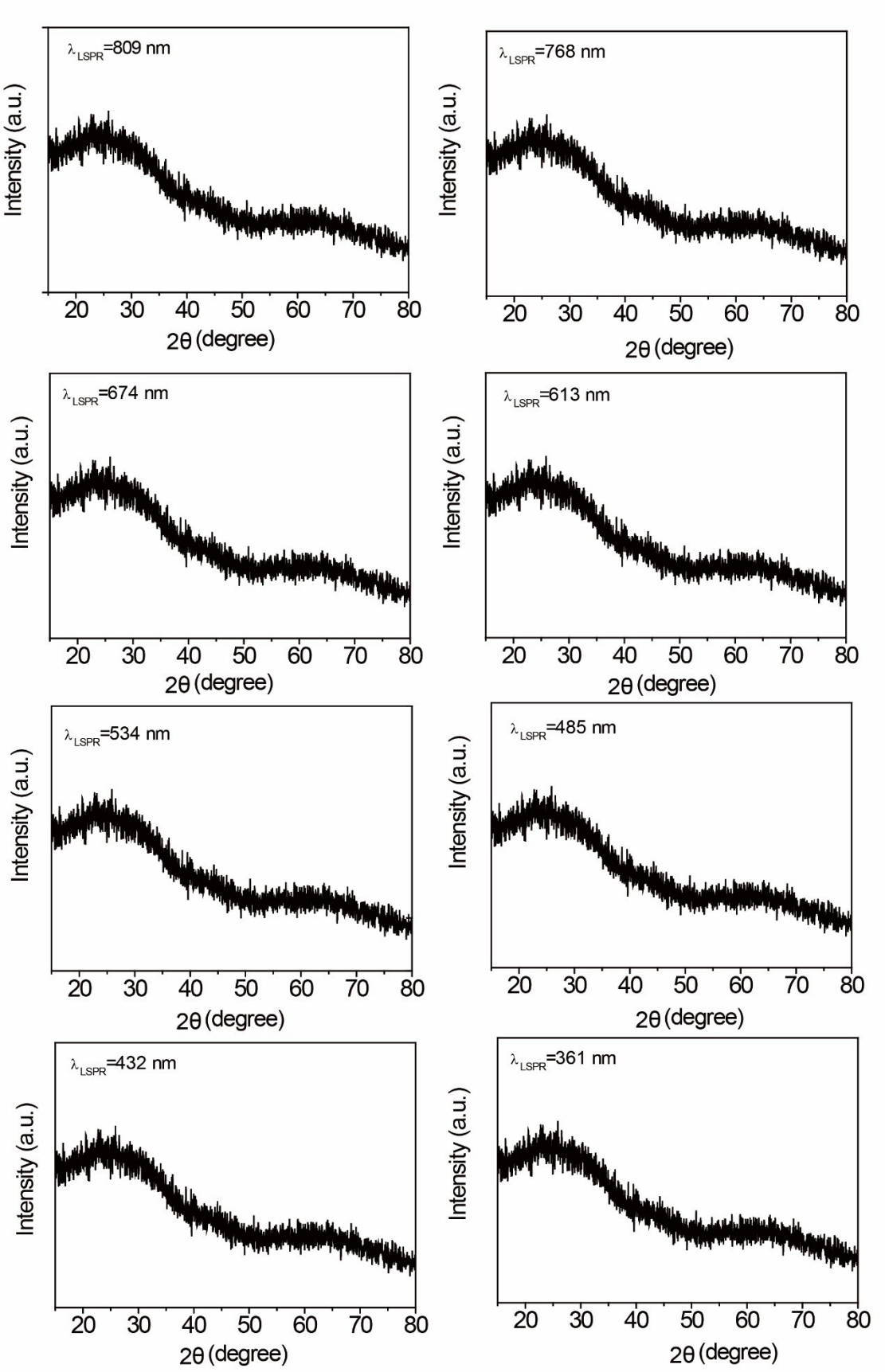

Fig. S12. XRD patterns of MoO_3 nanosheets with different LSPR peaks.

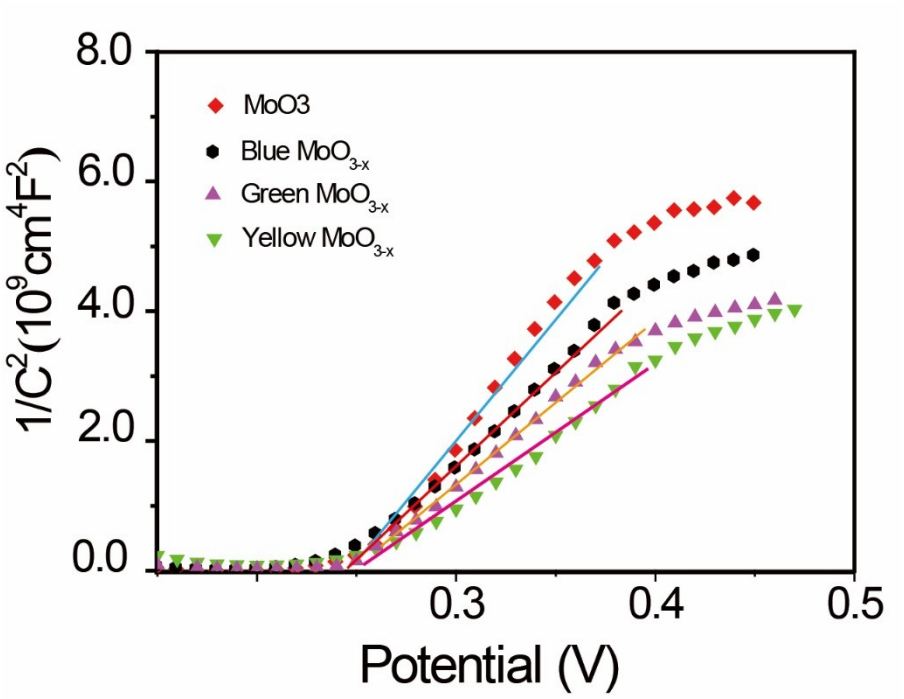

Fig. S13. Mott-Schottky plots of MoO_3 nanosheets and MoO_{3-x} nanosheets with different colors.

The charge carrier densities (N) of MoO_3 and MoO_{3-x} can be calculated by the following equation[S2]:

$$N= (2/e_0 \varepsilon \varepsilon_0) [d(1/C^2)/dV]^{-1}$$

where e_0 is the electron charge, ε is the dielectric constant of MoO_3, ε_0 is the permittivity of vacuum, C is the differential capacitance, and V is the applied bias at the electrode.

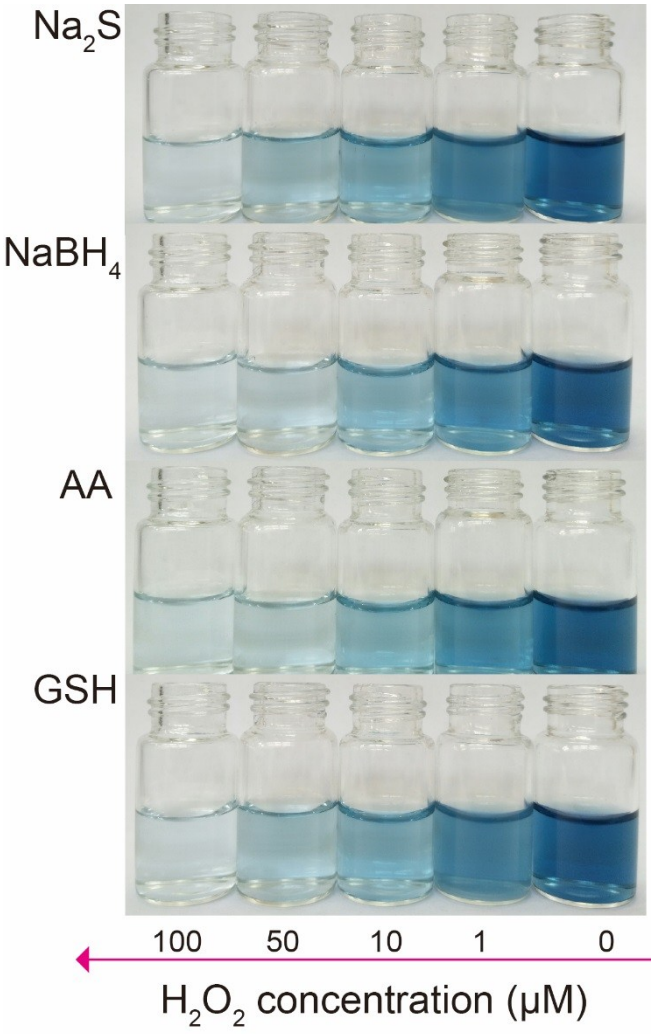

Fig. S14. Photographs of MoO_{3-x} nanosheet dispersion using different types of reducing agents in the absence and presence of H_2O_2 with different concentrations (1-100 μM), including Na_2S, $NaBH_4$, ascorbic acid (AA), and glutathione (GSH).

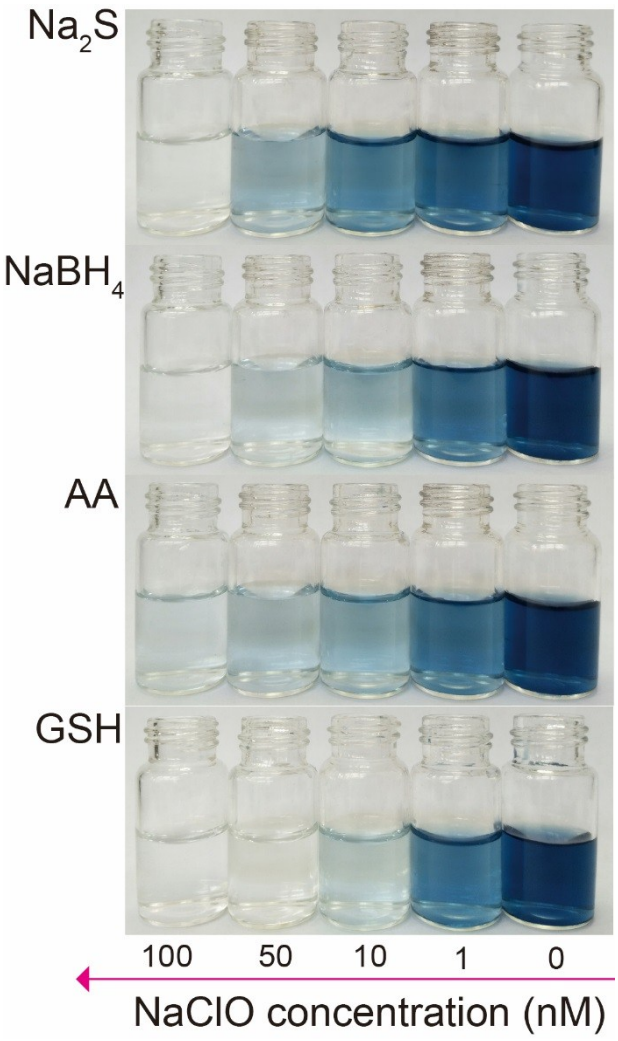

Fig. S15. Photographs of MoO_{3-x} nanosheet dispersion using different types of reducing agents in the absence and presence of NaClO with different concentrations (1-100 nM), including Na_2S, $NaBH_4$, ascorbic acid (AA), and glutathione (GSH).

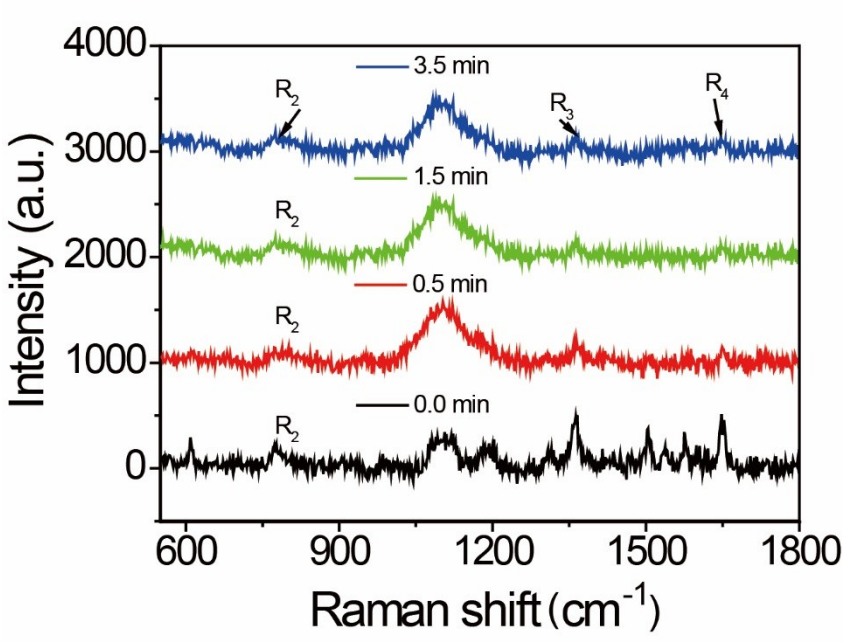

Fig. S16. Time-dependent SERS spectra of R6G adsorbed on the surface of blue MoO_{3-x}. The concentration of R6G is maintained at 1 fM.

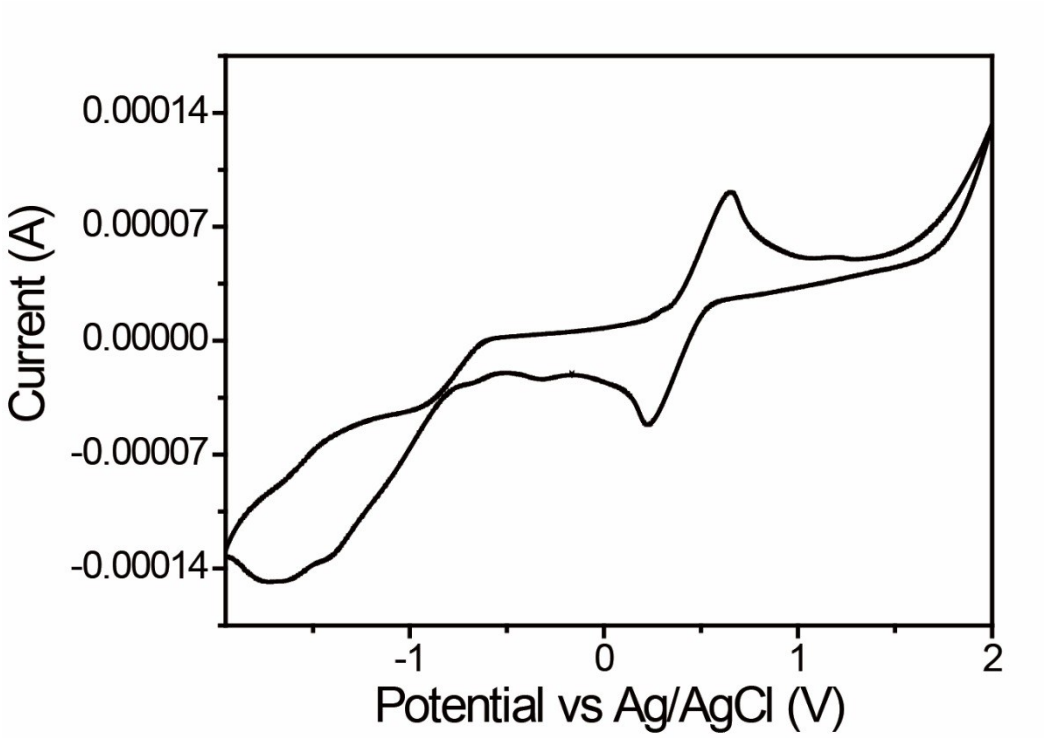

Fig. S17. Cyclic voltammogram of ferrocene in acetonitrile solution.

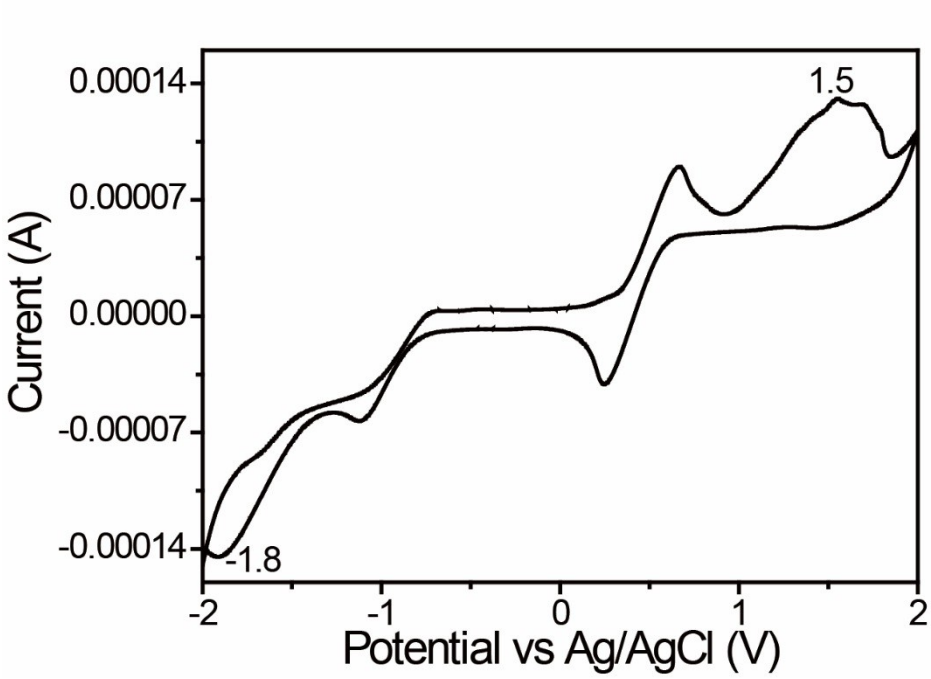

Fig. S18. Cyclic voltammogram of blue MoO_{3-x} nanosheet dispersion with ferrocene/ferrocenium (Fc/Fc^{+}) as the internal standard in acetonitrile solution.

The VB and CB of PDA-coated MoO_{3-x} nanosheets are calculated according to the following equations using the ferrocine as the internal standard[S3]:

$$E_{VB} = [\ -4.8 + E_{Fc/Fc+}{}^{1/2} - E_{ox}]\ eV$$

$$E_{CB} = [\ -4.8 + E_{Fc/Fc+}{}^{1/2} - E_{red}]\ eV$$

where VB and CB are valence band and conduction band, E_{ox} and E_{red} are oxidation and reduction potentials of PDA-coated MoO_{3-x} nanosheets, $E_{Fc/Fc+}{}^{1/2}$ is the average of oxidation and reduction potential of ferrocene.

[S1] L. Tao, K. Chen, Z. Chen, C. Cong, C. Qiu, J. Chen, X. Wang, H. Chen, T. Yu, W. Xie, S. Deng, J. Xu, *J. Am. Chem. Soc.* 2018, **140**, 8696-8704.

[S2] N. Zhang, A. Jalil, D. Wu, S. Chen, Y. Liu, C. Gao, W. Ye, Z. Qi, H. Ju, C. Wang, X. Wu, L. Song, J. Zhu, Y. Xiong, *J. Am. Chem. Soc.* 2018, **140**, 9434-9443.

[S3] S. Paul, S. Ghosh, B. Dalal, P. Chal, B. Satpati, S. De, *Chem. Material.* 2018, **30**, 5020-5031.